Physics of the Earth and Planetary Interiors 173 (2009) 162–170

Contents lists available at ScienceDirect

Physics of the Earth and Planetary Interiors

journal homepage: www.elsevier.com/locate/pepi

Paleomagnetic field variation with strong negative inclination during the Brunhes chron at the Banda Sea, equatorial southwestern Pacific

Yin-Sheng Huang[a,*], Teh-Quei Lee[b], Shu-Kun Hsu[a], Tein-Nan Yang[b]

[a] Institute of Geophysics, National Central University, Chung-Li, Taiwan
[b] Institute of Earth Science, Academia Sinica, Taipei, Taiwan

ARTICLE INFO

Article history:
Received 15 October 2007
Received in revised form 24 October 2008
Accepted 17 November 2008

Keywords:
Pacific Ocean
Geomagnetic field
Brunhes chron
Paleomagnetism
Inclination anomaly

ABSTRACT

We reconstruct the earth magnetic field in the Brunhes epoch at the Banda Sea by studying the paleomagnetic data from core MD012380, collected during the International Marine Global Change Study (IMAGES) VII Cruise in 2001. Magnetic analysis is carried out for whole core with a sampling spacing of 1 cm by using u-channel. Magnetic susceptibility (χ), nature remanent magnetization (NRM), anhysteretic remanent magnetization (ARM), and isothermal remanent magnetization (IRM) are measured in our paleomagnetic experiment. Results show the low latitude geomagnetic field variation at the Banda Sea during the last ~820 kyr. Except for the Brunhes/Matuyama boundary (BMB), there is no clear signal of reverse events in paleo- inclination and paleo-declination patterns. However, the synthetic paleointensity curve displays the asymmetrical saw-tooth pattern that can be used for determining reverse events, and shows a maximum intensity drop at the BMB. The characteristics of paleointensity provide a useful tool to identify reverse signals and improve the difficulties from only using inclination and declination patterns, especially at low latitude. With the help of paleointensity, inclination and declination, we have identified five reverse events. Furthermore if we consider the secular variation effect, we think that the strong negative inclination observed in our study may be the zonal time-averaged field with paleo secular variation, rather than non-dipole effect within the Brunhes epoch.

1. Introduction

Geocentric axial dipole (GAD) hypothesis is usually assumed in tectonic studies by using paleomagnetic data (McElhinny, 1973). Following this hypothesis, the averaged virtual geomagnetic pole (VGP) position should coincide with the geographic pole. However the existence of inclination anomaly in the central Pacific indicates that GAD model is not exactly correct. Therefore, zonal time-averaged field (TAF) models were proposed (Wilson, 1971; Wilson and McElhinny, 1974) and "inclination anomaly" is interpreted (Merrill and McElhinny, 1977; McElhinny et al., 1996). Because more reliable paleomagnetic data are accumulated, nonzonal TAF models using spherical harmonic analysis have been proposed (Gubbins and Kelly, 1993; Kelly and Gubbins, 1997; Johnson and Constable, 1995, 1997; Kono et al., 2000). Paleo secular variation (PSV) effects are also involved in order to consider dipole wobble, intensity variation in the main dipole and the non-dipole component (Cox, 1970). Hatakeyama and Kono (2001) have demonstrated that the paleomagnetic data is strongly influenced by PSV. They proposed that TAF and PSV models are indeed coupled so that both models should be taken into account to describe the earth's TAF characteristic (Hatakeyama and Kono, 2002). Recently, Johnson et al. (2008) have investigated the 0–5 Ma geomagnetic fields recorded by combining global data sets from lava flow. They suggested that the characteristic of zonal structure in PSV and the TAF is different during normal and reverse polarity chrons over the past 5 Ma.

Besides, the geomagnetic field reversal is also an important factor of the geomagnetic field. Reverse events are usually observed and identified by using angular variation of paleomagnetic data (inclination and declination) (e.g. Champion et al., 1988). In order to get high resolution paleomagnetic data, long time deposition and undisturbed strata are often necessary. However, because the range of inclination variation is large near the equator (i.e. from 0° to ±90°) (Valet et al., 1989) and declination is not oriented in most marine sediment cores, it is hard to observe reversal signals by using paleo-inclination and paleo-declination. Until last decade, the method of simulated relative paleointensity (RPI) has been well developed (Tric et al., 1992; Guyodo and Valet, 1996, 1999). It provides a way to determine polarity reversal during the past 800 kyr by using the RPI variation, and becomes easier to rebuild the geomagnetic field in more detail.

In this study we present the high resolution paleomagnetic data from core MD012380, collected at the Banda Sea during the International Marine Global Change Study (IMAGES) Cruise VII in 2001. The

* Corresponding author.
E-mail address: yinson@gmail.com (Y.-S. Huang).

0031-9201/$ – see front matter © 2008 Elsevier B.V. All rights reserved.
doi:10.1016/j.pepi.2008.11.013

aim of IMAGES Cruise VII is to understand the paleo-environment change in the western Pacific Ocean. Situated at the western Pacific warm pool near the equator, the core MD012380 is important for studying the paleo-environment change which is affected by the warm pool and Inter-tropical Convergence Zone (ITCZ). In order to carry out the study, the most important work is to calibrate the core age. Thus, we combine paleomagnetic data with isotope data (δ^{18}O and ^{14}C) of core MD012380 to establish an age model. We also determine some reverse events and rebuild the geomagnetic field at the Banda Sea. Because the paleo-inclination and paleo-declination patterns show no clear reversal signals in the study, we use the RPI variation to identify reverse events alternatively. Furthermore we discuss the phenomenon of strong negative inclination found in our data by combining paleomagnetic data in the central and southwestern Pacific (Elmaleh et al., 2001). If the TAF model with paleo secular variation is considered (Hatakeyama and Kono, 2002), we think that the strong negative inclination may be the TAF domination instead of non-dipole effect.

2. Geology and sampling

The Banda Sea basin is a marginal basin whose maximum depth exceeds 5000 m (Fig. 1), and can be divided into two main portions (North and South Banda basins) by the Banda Ridges (Honthaas et al., 1998). It is located within an area where the Pacific, Eurasian and Indo-Australian plates have been converging since Mesozoic times (Hamilton, 1979; Jolivet et al., 1989). There are several hypotheses to explain the origin and mechanism of the Banda basin. In the early days, the Banda basin, Celebes basin and Sulu basin were considered as a trapped piece of Cretaceous–Eocene oceanic crust (Lee and McCabe, 1986). However, the South Banda basin was thought to be a back-up basin opening during late Tertiary times based on the point of geodynamic view (Hamilton, 1979; Nishimura and Suparka, 1990; Hinschberger et al., 2001). The spreading age was believed to be late Miocene to early Pliocene times (about 6.5–3.5 Ma) (Hinschberger et al., 2001).

Core MD012380 was drilled at 5°45.64′S and 126°54.25′E near the Banda Ridge at a depth of about 3232 m (Fig. 1). Total length of the core is 39.9 m. There was no core orientation procedure while drilling so that the true declinations of the samples could not be obtained. There is also no screwing, bending or deforming appeared in the core. All specimens were sampled by using u-channel with a length of 1.5 m. Most sediments are mainly composed of clay and silty clay with spotted pyrite, organic and glauconite spots. Clay compositions are dominated by nanno oozes with foraminifers and diatoms (Bassinot and Baltzer, 2001). There are only few bio-disturbances in core MD012380 so that it could provide a good data for paleomagnetcic analysis.

3. Analysis

3.1. Experimental procedures

In order to ensure that there was no external effect of magnetic components during measurement, all experiments of our study were performed in the magnetic shielded room at the Paleomagnetic Laboratory, Institute of Earth Science, Academia Sinica, Taiwan. Samples with u-channel from core MD012380 were sequential and discrete measuring with 1 cm spacing. Bartinton MS-2 magnetic susceptibility meter was used to measure the bulk magnetic susceptibility (χ). Detailed alternating field (AF) demagnetization processes were done by using the 2G 755 SRM Superconducting Quantum Interference Device (SQUID). Basic measuring procedure is as follows. (1) Measure magnetic suscep-

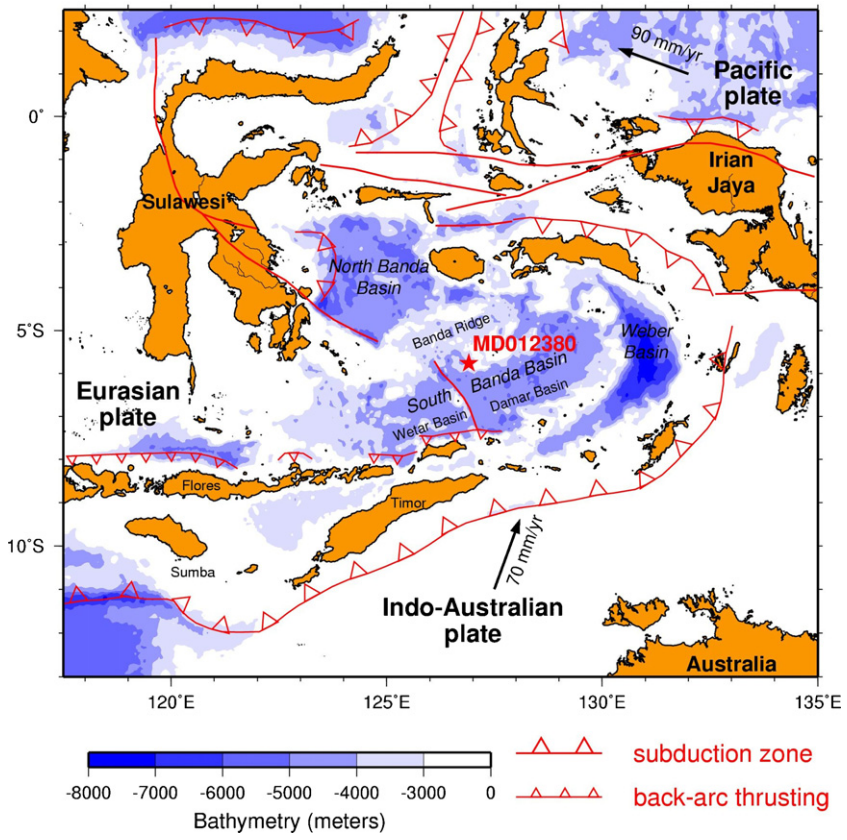

Fig. 1. Topography and structure map of the Banda basin. Star symbol is the core site of MD012380. The black arrows represent the relative motion velocity between the Indo-Australian plate, Pacific plate and Eurasian plate.

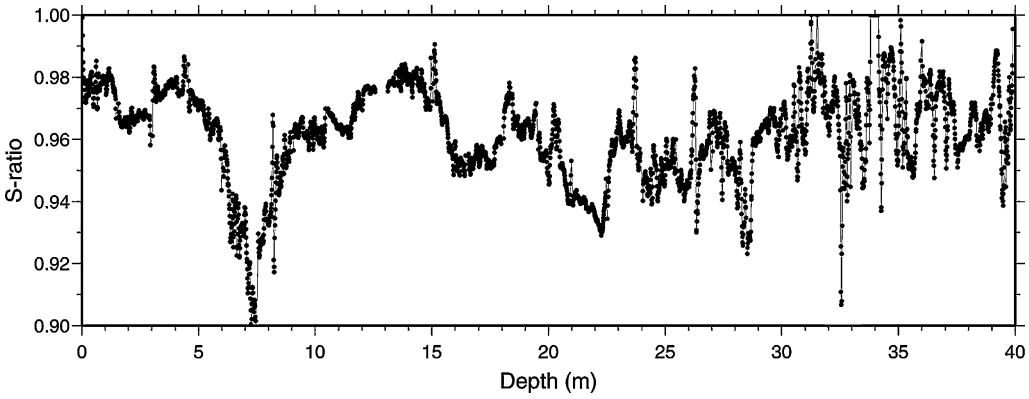

Fig. 2. S-ratio data of core MD012380.

tibility. (2) Nature remanent magnetization (NRM) was applied stepwise to AF demagnetization from 0 mT to 100 mT with an increment of 10 mT field. (3) Anhysteretic remanent magnetization (ARM) was acquired in a 0.1 mT stable field within a 100 mT alternating field, and then measured every 10 mT field with AF demagnetization from 0 mT to 60 mT. (4) All demagnetized samples were tested for high coercivity magnetization components by using isothermal remanent magnetization (IRM). A spiral coil magnetizer was used to produce the IRMs with peak fields of 25 mT, 50 mT, 75 mT, 100 mT, 150 mT, 200 mT, 250 mT, 300 mT, 500 mT, 750 mT and 950 mT.

3.2. Magnetic mineral properties

For paleomagnetic studies, especially for the RPI simulation, it is important to verify whether the core sediments are suitable for the study or not. Properties of RM carrier must be analyzed to check that RM carrier is linearly related to the Earth's magnetic field intensity. Depending on the result of S-ratio data (in our study, S-ratio is defined as $IRM_{-0.3T}/IRM_{0.95T}$), we find that S-ratio of core samples mostly varies between 0.94 and 1.00, and drops to 0.9 only at the interval between 7 m and 8 m (Fig. 2) which may be induced by environmental changes. It reveals that magnetic minerals of our samples are mainly dominated by magnetite and there are only minor magnetic minerals with high coercivity found in the core MD012380. Therefore, RMs of our study should be mostly carried by magnetite.

Moreover, a plot of ARM versus χ which represents grain size variation of magnetite (King et al., 1982) is shown for core MD012380 in Fig. 3. Results indicate that grain size of magnetite is mainly distributed between 0.1 μm and 5.0 μm (i.e. single-domain and pseudo-single-domain). For the best RPI simulation, Tauxe (1993) had suggested that the magnetization of sediments should be carried by magnetite, preferably in single and/or pseudo-single-domain grain size. It appears that sediments of core MD012380 are suitable for the RPI analysis.

In order to check the possibility of physical re-alignment of magnetic grains, anisotropy of magnetic susceptibility analysis has been applied. Most magnetic fabrics revealed that K_{min} axes are perpendicular to the deposition plane (K_{min} is greater than 80°). Thus, there is no re-alignment of magnetic grains occurred during coring and sampling in the study.

3.3. Paleo-inclination and paleo-declination

According to the demagnetization results of NRM, the characteristic remanent magnetization (ChRM) and the stability of RM can be analyzed by using the Zijderveld diagram (Zijderveld, 1967). The ChRM, including D–N and N–E components, should theoretically regress towards the origin in orthogonal coordinate after AF demagnetization steps. Indeed, some D–N components in our study decrease linearly with a small intercept from the origin (e.g. samples 330, 1242 and 3112 in Fig. 4). The phenomenon might be due to some high coercivity magnetic minerals co-existing with magnetite in the core. From the results of SIRM, we can also find that they are not entirely saturated at 300 mT (Fig. 5). It proves that the existence of the high coercivity components in these samples. Because the AF demagnetications of NRM were only processed up to 100 mT in our experiment, some of these high coercivity components could not be sufficiently removed. It might be the reason that the D–N components did not converge to the origin. However, both D–N and N–E components are linearly regressed, and N–E components still converge to the origin after demagnetization steps. Furthermore, most NRM are less than 50% left after 40 mT field demagnetization step and down to less than 1/10 of original NRM after 60 mT (Fig. 4). It indicates that our analysis of ChRM is stable and reliable for judging the angular variation of the geomagnetic field.

Besides, westward drifting component of the VGP is also an important factor to induce periodical variation in the geomagnetic field. In order to get information about true reversal signals, it is necessary to eliminate the influence of this factor. Because the core site of MD012380 is near the equator (5°45.64′S), the maximum range of inclination variation caused by westward drifting of the VGP is

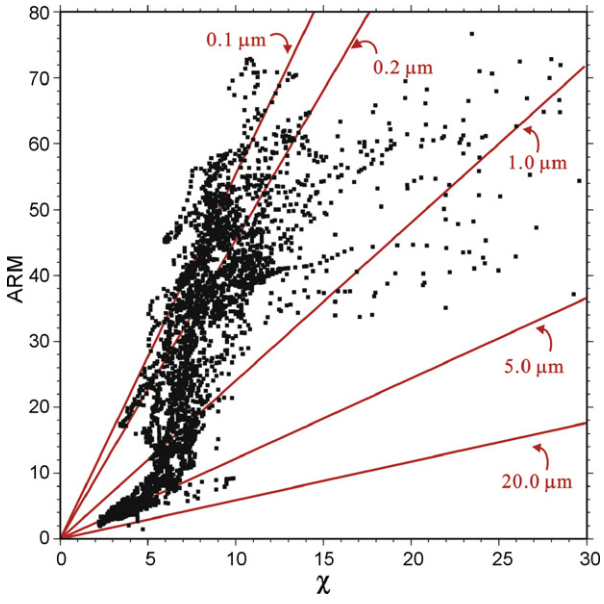

Fig. 3. ARM versus χ diagram which represents grain size variation of magnetite.

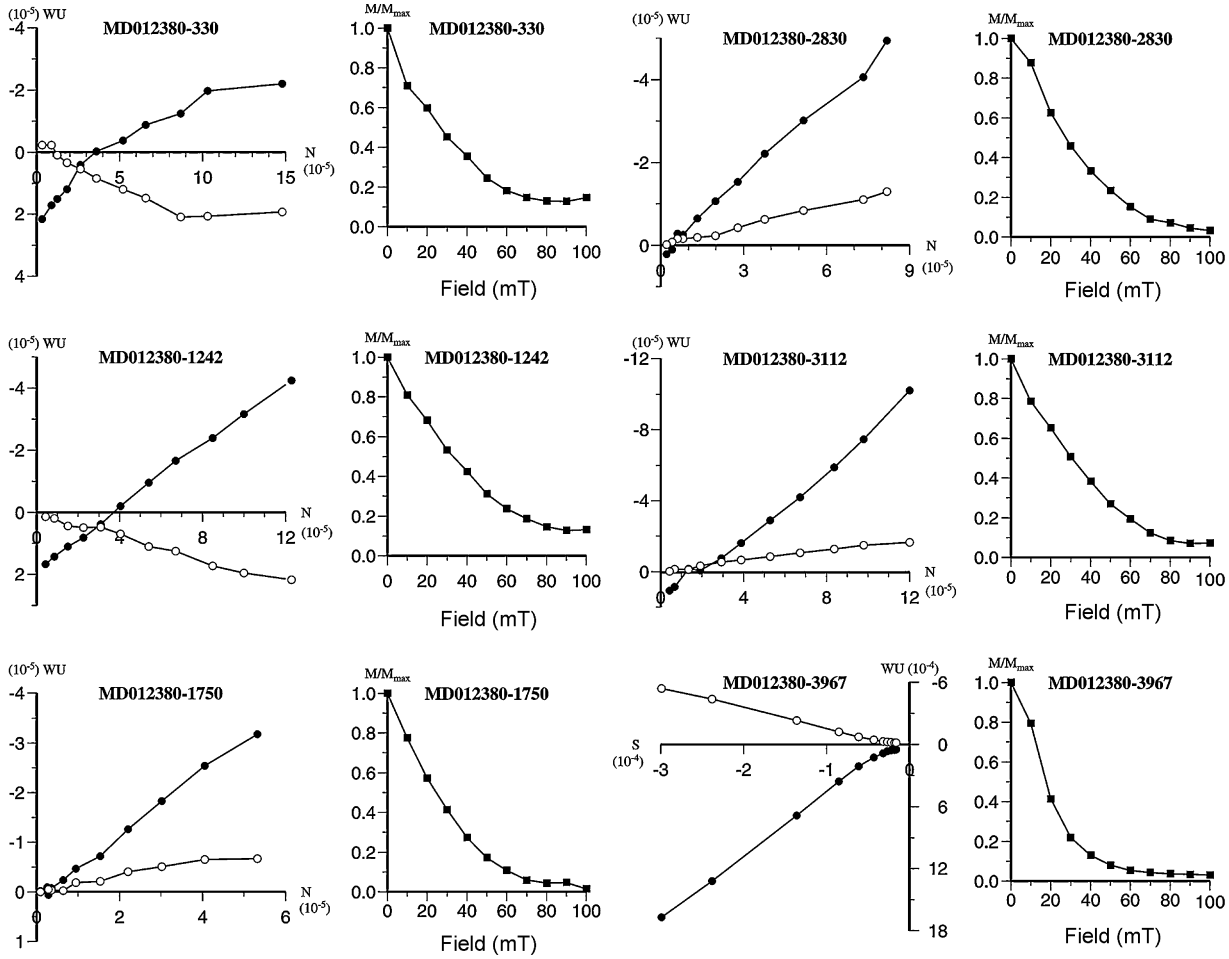

Fig. 4. Typical orthogonal diagrams and AF demagnetization curves of the studied samples during stepwise AF demagnetization of the NRM. (solid circle: D–N component; open circle: N–E component).

estimated to be about −40° to +10° in our study. Angular variation within the range may be explained as the VGP drifting rather than polarity reversal. Only when variation exceeds the range, it may be considered as a reversal signal. Base on the estimation, reverse events could be identified.

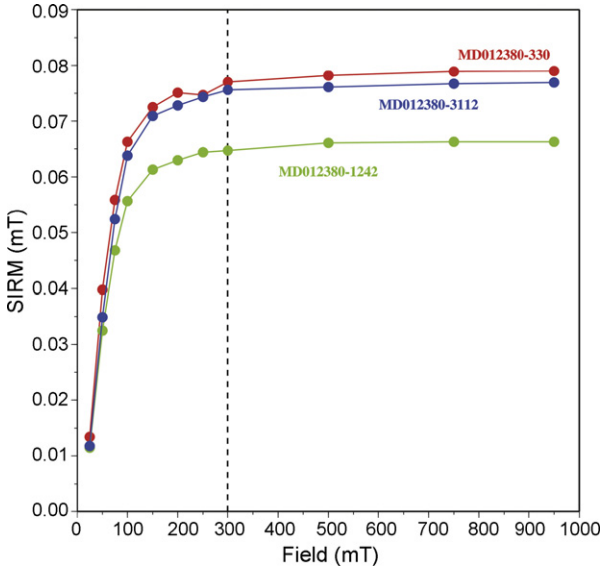

Fig. 5. SIRM results of studied samples.

3.4. Relative paleointensity (RPI) simulation

NRM acquired during deposition would exponentially decay as time elapsing, so it is difficult to obtain original paleointensity value. Until last decade, the experimental method to simulate RPI variation had been well developed (Tric et al., 1992; Guyodo and Valet, 1996, 1999). Tric et al. (1992) simulated RPI by using NRM normalized with ARM, SIRM and χ (NRM and ARM are applied with 20 mT AF demagnetization step) in order to find the best way to remove the effects of magnetic lithology. They found that these parameters seemed to be equally well to normalize the NRM intensity. But they preferred to propose that identical treatment on NRM and ARM demagnetization would offer the best information about magnetization being carried by similar families of grain. Based on the method, Guyodo and Valet (1999) compiled a set of data to establish the simulation intensity pattern of the earth's magnetic field during the past 800 kyr (Sint-800).

In our study, NRM is normalized by ARM, SIRM and χ (NRM and ARM are applied with AF demagnetizing step of 20 mT), and these obtained ratios are compared in order to determine whether they are suitable for the RPI study or not. The comparison results show that NRM_{20mT}/ARM_{20mT}, NRM_{20mT}/SIRM and NRM_{20mT}/χ reveal similar patterns (Fig. 6). Cross-correlation analysis displays a positively correlated and coherent test show good coherence (greater than 0.7) between these parameters. Therefore, they may provide the equivalent estimations for the RPI study. To compare with the Sint-800, we adopt the NRM_{20mT}/ARM_{20mT} as a proxy to simulate

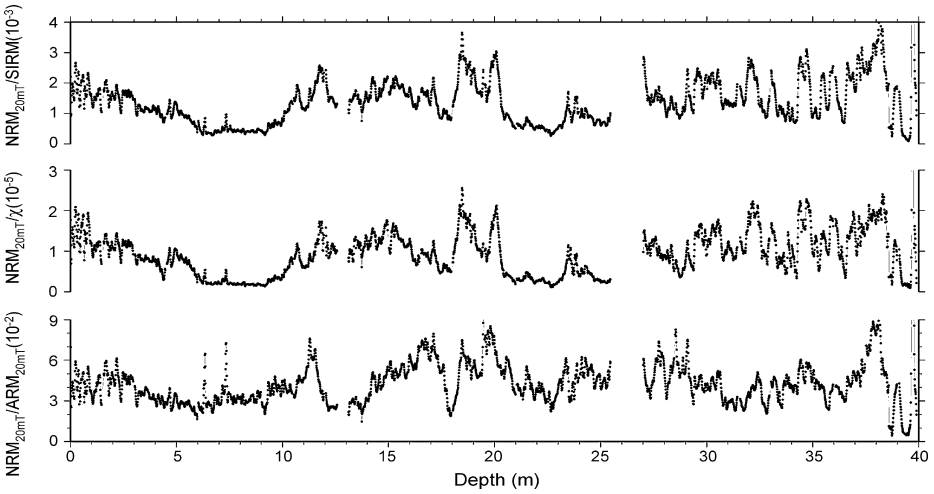

Fig. 6. Three estimation of the RPI for core MD012380; NRM_{20mT}/SIRM, NRM_{20mT}/χ and NRM_{20mT}/ARM_{20mT}.

RPI in the study. However, the proxy only represents the relative intensity variation at the study area instead of true VGP moment.

4. Results

4.1. Age control and age model

Our result of RPI variation displays the asymmetrical saw-tooth pattern and shows intensity decrease in some segments of the core. Especially, the maximum drop is near the bottom (Fig. 7(a)). Valet and Meynadier (1993) reported that geomagnetic intensity exists an asymmetrical saw-tooth pattern, which intensity decreases gradually during the intervals of stable polarity and recovers immediately after a polarity change. Therefore, the variations in our paleointensity pattern may be dominated by the reverse events or excursions. Accordingly, we principally used this parameter to identify reverse events. Guyodo and Valet (1999) had shown the simulated intensity variation of the geomagnetic field during the last 800 ka (Sint-800; Fig. 7(b)). Comparing our paleointensity result with the Sint-800, some correlations could be obtained. We found similar variation pattern of the paleointensity curve, including the asymmetrical saw-tooth pattern. The feature provided a basis for further age calibration. According to the correlation, we correlated seven "depth-to-age" points (Fig. 7) to convert intensity variation of depth into age (Fig. 7; Table 1).

Besides the RPI dating, AMS ^{14}C dating and $\delta^{18}O$ stratigraphy analysis were also available in the upper part of the core MD012380 for providing more age control (Chen, 2002). For carbon isotope

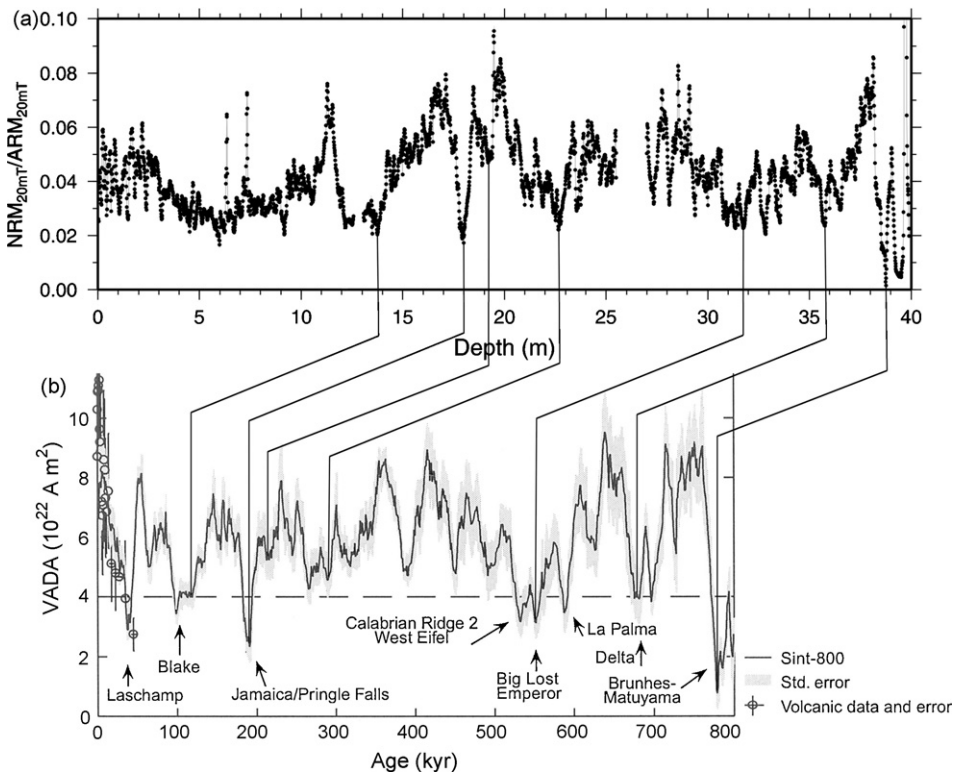

Fig. 7. (a) shows the result of RPI (NRM_{20mT}/ARM_{20mT}) as functions of depth. (b) is the Sint-800 pattern. Lines correlated a with b show the relations between our paleointensity data and the Sint-800.

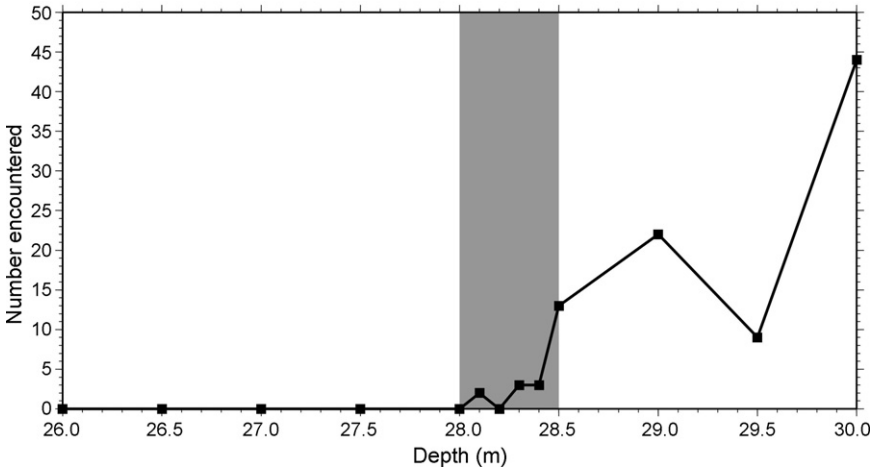

Fig. 8. Distribution of the *Pseudoemiliania Lacunosa* at interval 26–30 m. Gray area shows the large extinction location of the *Pseudoemiliania Lacunosa* whose depth is at interval 28–28.5 m.

dating, specimens of planktonic foraminifera *Globigerinoides Sacculifer* and *Globigerinoides ruber* were picked from five depths of core MD012380. These samples (>3.0 mg) were sent to Rafter Laboratory, Institute of Geological and Nuclear Science, New Zealand, for ^{14}C accelerator mass spectrometry (AMS) dating. *Globigerinoides Saccculifer* was also picked from 300 μm to 355 μm size fraction for oxygen isotope analysis. All specimens were immersed in methanol and applied to ultrasonic vibration for 5 s (three times). Afterward they were immersed in NaOCl for 24 h, cleaned by de-ionized water (five times) and then dried. Finally specimens were reacted with 100% H_3PO_4 at 90 °C about 50 min and applied with Micromass spectrometer to determine $\delta^{18}O$ values. The precision of the measurements for $\delta^{18}O$ was better than 0.02‰ (Chen, 2002).

Results of $\delta^{18}O$ data were correlated against the low latitude stack (Bassinot et al., 1994) in order to obtain an age model for the upper part of core MD012380. Depths and corresponding ages of these controlling points are listed in Table 1. In total, 14 isotope dating points, including five of ^{14}C and nine of $\delta^{18}O$ dating analysis were obtained (Chen, 2002). Moreover, because there was no control point at the interval from 22.75 m to 31.81 m, a nannofossil analysis was then performed. Last appearance (LA) of the *Pseudoemiliania Lacunosa* was found at the interval of 28–28.5 m (Fig. 8) and its extinctive age was given about 458 ka (Berggren et al., 1995).

All above control points (22 in total) are used to establish the age model for this study (Table 1). Result shows that core MD012380 covers the past ~820 ka with a total depth of 39.9 m, and average sedimentation rate is estimated to be about 4.9 cm/kyr. Age model is interpolated by all control points and is closed to a curve of quadratic equation (Fig. 9). It indicates that there is higher compaction ratio of sediments in the deeper part of the core.

4.2. Geomagnetic field variation

On the basis of the constructed "depth-to-age" relationship, we can convert the depth of the paleomagnetic parameters (paleointensity, paleo-inclination and paleo-declination) into age (Fig. 10). The clearest angular variation of inclination and declination, and the maximum drop of paleointensity are found between 780 ka and ~820 ka. We believe that these features are significant in judging the Brunhes/Matuyama Boundary (BMB) near the equator and its age is given 780 ky (Cande and Kent, 1995).

Table 1
Age model of the core MD012380.

Depth (cm)	Age (ka)	Method
41	4.17	^{14}C
111	7.71	^{14}C
191	14.55	^{14}C
301	18.34	^{14}C
411	23.63	^{14}C
461	34	$\delta^{18}O$
851	65	$\delta^{18}O$
971	78	$\delta^{18}O$
1051	86	$\delta^{18}O$
1261	106	$\delta^{18}O$
1384	119	RPI
1451	126	$\delta^{18}O$
1501	134	$\delta^{18}O$
1571	150	$\delta^{18}O$
1681	164	$\delta^{18}O$
1805	193	RPI
1937	214	RPI
2275	290	RPI
2840	458	LA of Lacunosa
3181	552	RPI
3589	677	RPI
3870	780	RPI

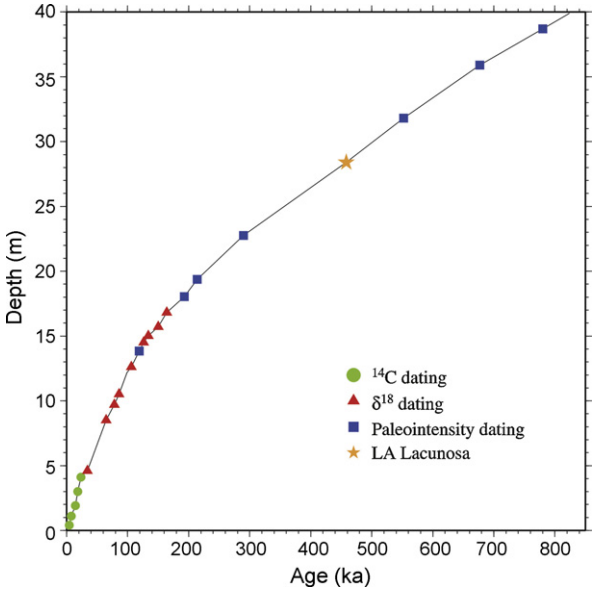

Fig. 9. Age model of the core MD012380.

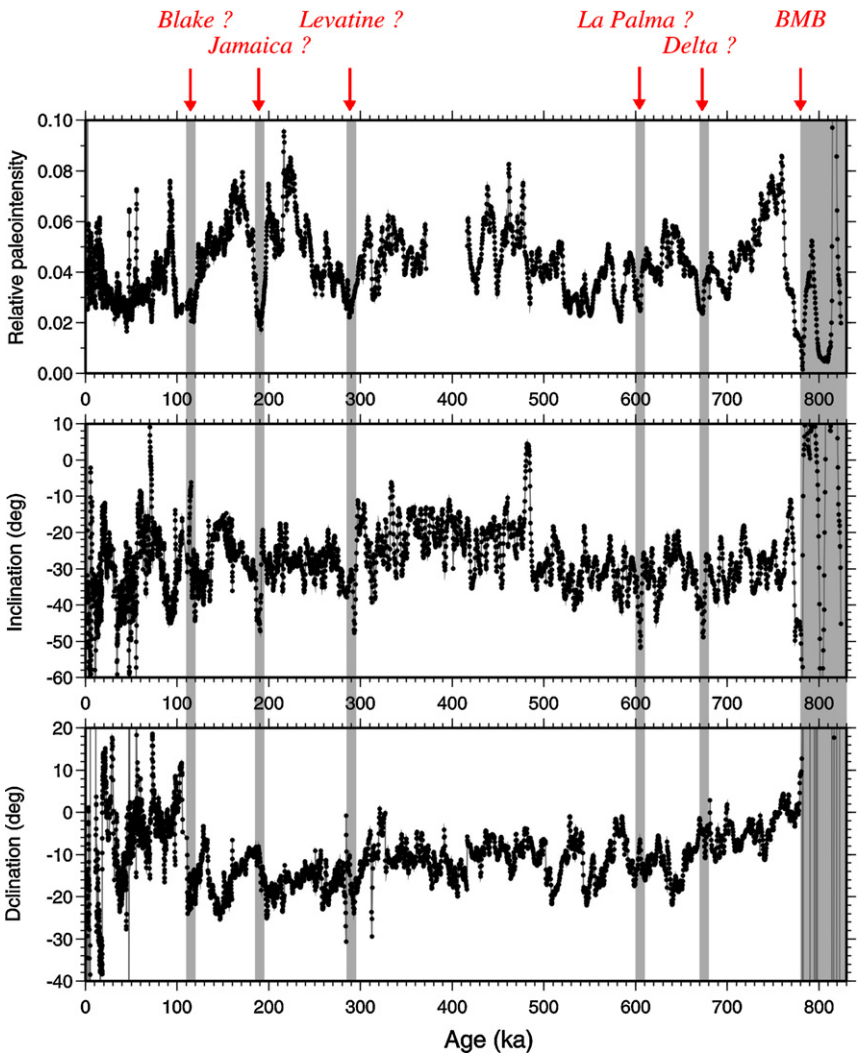

Fig. 10. (a)–(c) represent the paleomagnetic results of the RPI, inclination and declination. Gray area shows the determined reverse events in the Brunhes epoch.

Except for the BMB, there are some slight angular variations in inclination and declination patterns, but we could not distinguish the effect between polarity reversal and secular variation. Similar patterns are also found in some paleomagnetic studies at low latitude, such as at the South China Sea (Lee, 1999) and the Sulu Sea (Schneider and Mello, 1996). Nevertheless, reverse events could be detected by observing RPI decrease during the Brunhes chron (Guyodo and Valet, 1999). It provides an effective method to determine the geomagnetic field reversal, especially near the equator or at low latitude. Finally, we identify five reverse events, including the Delta Event, La Palma Event, Levatine Event, Jamaica Event and Blake Event (Fig. 10). Corresponding depths versus ages of these events are arranged in Table 2. The variation pattern of the RPI in our study is similar to the Sint-800, and dating ages of these events are in good accordance with the past studies (Ryan, 1972; Champion et al., 1988; Valet and Meynadier, 1993).

Table 2
Corresponding depth versus age of reverse events in the study.

Depth (m)	Polarity subchrons	Age (ka)
38.7	B/M Boundary	780
35.6–36	Delta event	668–679
33–33.7	La Palma event	590–610
22.5–23	Levatine event	285–297
17.8–18.2	Jamaica event	186–195
13.1–14	Blake event	111–120

5. Discussion

According to the GAD hypothesis (McElhinny, 1973) and the zonal TAF model (Merrill and McElhinny, 1977; McElhinny et al., 1996), mean inclination near the equator should be close to 0°. However we found that mean inclination at the Banda Sea is about −28° which is greater than the theoretical value. Elmaleh et al. (2001) had also shown the persistence of the strong negative inclination of the geomagnetic field in the central and southwestern Pacific Ocean. What may be the reasons for the phenomenon in this area? Doell and Cox (1972) suggested a “Pacific non-dipole low” which was caused by a weak non-dipole field. Gubbins and Kelly (1993) concluded that non-axial dipolar feature might be induced by thermal anomalies in the deeper mantle. Johnson and Constable (1995) proposed that the central Pacific is dominated by large negative inclination anomalies with a significant non-axial dipolar contribution.

However, if we consider that the VGP position does not coincide with the geographic pole but varies with time, the PSV effect should be involved. Hatakeyama and Kono (2001) had demonstrated that the mean direction of the paleomagnetic data is strongly influenced

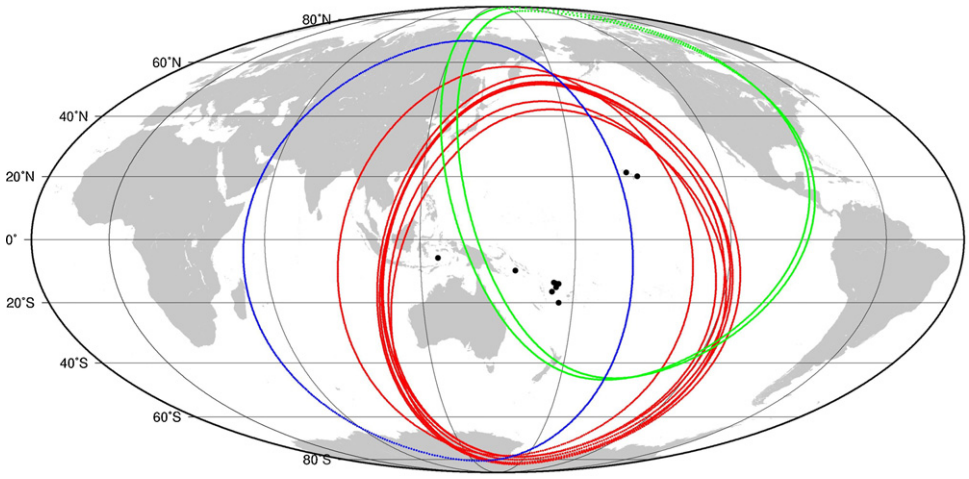

Fig. 11. Co-latitude (small circles) for all used sites (arranged in Table 3). Red circles are small circles of core sites in the Southern Hemisphere; blue one shows that for core MD012380; green ones represent those in the Northern Hemisphere. (For interpretation of the references to color in this figure legend, the reader is referred to the web version of the article.)

by PSV, and proposed a new TAF model with PSV for the last 5 My (Hatakeyama and Kono, 2002). Recently, Johnson et al. (2008) combined a series of global data from lava flows and suggested that polarity asymmetries in PSV and TAF may be related to the long-lived core-mantle boundary conditions on core flow. Therefore, if we take PSV effect into account, the VGP should be located at some high latitude of the Earth, instead of coinciding with the geographic pole.

Mean value of inclination (I_{mean}) of core MD012380 is about -28° which is similar to the present day value and ΔI is estimated about -16.8° ($\Delta I = I_{mean} - I_{GAD}$). It seems that there is also strong negative inclination in our study area. In order to clarify the phenomenon, we combine our data with past study from central and southwestern Pacific (Elmaleh et al., 2001) (Table 3) and try to locate the VGP position. Because the characteristic of PSV and the TAF are different during normal and reverse polarity chrons over the past 5 Ma (Johnson et al., 2008), all selected data are younger than 780 ka (i.e. within the Brunhes normal epoch). In Table 3, we can find that all ΔI show strong negatives values and range is between -10° and -20° in the central and southwestern Pacific in the Southern Hemisphere (SH).

According to these paleo-inclination data (Table 3), we can estimate the paleomagnetic co-latitude for each site. Because it is difficult to obtain the real value of paleo-declination from marine sediment cores, we cannot determine the exact VGP position. In order to get a possible VGP location, we draw a small circle of paleomagnetic co-latitude base on the inclination data for each site (Fig. 11). The red circles represent the small circles of these sites at the SH, the blue one shows that from core MD012380, and the green ones are those in the Northern Hemisphere (NH) (Fig. 11). Although we do not know the exact VGP location, we can still propose the possible VGP position in the SH by combining the intersections of these small circles (Fig. 12). The estimated VGP position is located at about 80°S, which is close to the latitude of the present geomagnetic south pole calculated based on the International Geomagnetic Reference Field (IGRF) model. It is notice that the green small circles may represent the location of VGP in the NH hence there is no overlap near the estimated VGP area in the SH. Base on our results, we suggest that the averaged VGP location is at about 80°S instead of coinciding with the geographic pole within the Brunhes normal epoch (Fig. 12).

Accordingly, if we assume the zonal TAF model and accepted that the VGP varies around 80°S, the degree of the magnetic equator would be higher than the geographic equator during the Brunhes normal epoch. Then we will get the negative inclinations in the central and southwestern Pacific naturally. Therefore, instead of the non-dipole effect, we think that the reason of the strong negative

Table 3
Core site, age, mean inclination and ΔI used in the study.

Core	Site Latitude N	Site Longitude E	Age (Ma)	I_{mean} (°)	ΔI (°)
Ha1	20.10	−154.03	<0.78	42.3	6.10
Ha2	21.35	−158.18	<0.78	39.9	1.78
So2	−9.76	156.83	<0.20	−38.9	−19.50
Fil-a	−13.97	173.95	<0.59	−37.7	−12.80
Fil-b	−13.83	172.83	<0.61	−41.4	−14.90
Fil-c	−13.52	171.97	<0.55	−43.1	−17.30
Fi2	−15.06	173.00	<0.78	−40.6	−12.10
Fi3	−16.50	171.53	<0.78	−47.0	−16.10
Fi4	−20.06	174.36	<0.54	−46.2	−9.96
MD80	−5.76	126.90	<0.78	−28.2	−16.80

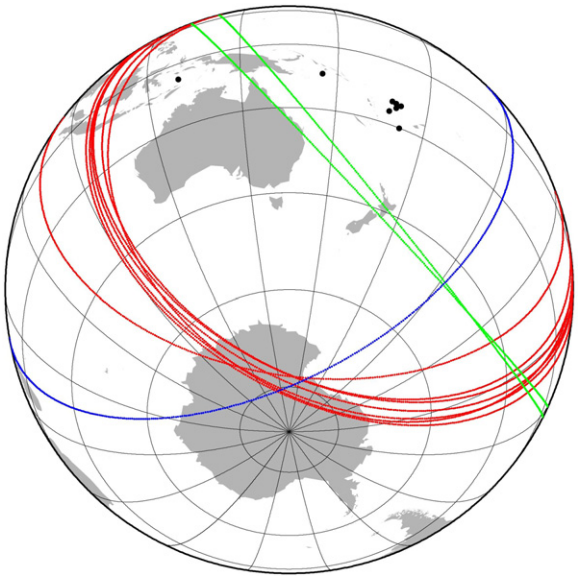

Fig. 12. Intersection of all small circles in the Southern Hemisphere. The estimated VGP area is at about 80°S during the Brunhes normal epoch. (For interpretation of the references to color in this figure legend, the reader is referred to the web version of the article.)

inclination in this area may be due to a time-averaged field effect with the paleo secular variation.

6. Conclusion

The core MD012380, obtained at the Banda Sea, records the past 820 kyr geomagnetic field (across BMB) and the average sedimentation rate is estimated to be 4.9 cm/kys. Five reverse events are identified during the Brunhes epoch in this study. There is no obvious angular reversal signal during the Brunhes epoch except for the BMB. In contract with the inclination and declination patterns, paleointensity varies as an asymmetrical saw-tooth pattern and the maximum intensity decrease occurs at the BMB. Although inclination and declination provides less evidence to detect reverse events near the equator, paleointensity is demonstrated to be an effective proxy. The simulated RPI shows an advantage in identifying polarity reversal and offers an opportunity to examine the geomagnetic field properties at low latitude.

Acknowledgements

We would like to appreciate to all the researchers and staffs on the *Marion Dufresne* during IMAGES Cruise VII for their good job in collecting core data at the Banda Sea site. For sampling the core, we acknowledge the Core Laboratory at the National Taiwan Ocean University, funded by National Science Council, Taiwan. We also thank members of Paleomagnetic Laboratory, Academia Sinica for help on experiments and members at Marine Geophysics Laboratory, National Central University for discussion. This research was supported by the National Science Council number NSC91-2611-M-001-003-IM. The figures were mainly plotted with the GMT software (Wessel and Smith, 1998).

References

Bassinot, F.C., et al., 1994. The astronomical of climate and the age of the Brunhes-Matuyama magnetic reversal. Earth Planet. Sci. Lett. 126, 91–108.
Bassinot, F.C., Baltzer, A., 2001. On board report of WEPAMA cruise MD122/IMAGES VII, P.133.
Berggren, W.A., et al., 1995. Late Noegene chronology: new perspectives in high-resolution stratigraphy. GSA Bull. 107 (11), 1272–1287.
Cande, S.C., Kent, D.V., 1995. Revised calibration of the geomagnetic polarity timescale for the Late Cretaceous and Cenozoic. J. Geophys. Res. 100 (B4), 6093–6095.
Champion, D.E., Lanphere, M.A., Kuntz, M.A., 1988. Evidence for a new geomagnetic reversal from lava flows in Idaho: discussion of short polarity reversals in the Brunhes and late Matuyama polarity chrons. J. Geophys. Res. 93, 11667–11680.
Chen C.W., 2002. The record of oxygen isotope stratigraphy during Quaternary in the Western Pacific Warm Pool. Master's thesis, National Taiwan University, Taipei, P.60. (in Chinese).
Cox, A.V., 1970. Latitude dependence of the angular dispersion of the geomagnetic field. Geophys. J. R. Astr. Soc. 20, 253–269.
Doell, R.R., Cox, A.V., 1972. The Pacific geomagnetic secular variation anomaly and the question of lateral uniformity in the lower mantle. In: The Nature of the Solid Earth. McGraw-Hill, New York, pp. 245–285.
Elmaleh, A., Valet, J.-P., Herrero-Bervera, E., 2001. A map of the Pacific geomagnetic anomaly during the Brunhes chron. EarthPlanet. Sci. Lett. 193, 315–332.
Gubbins, D., Kelly, P., 1993. Persistent patterns in the geomagnetic field over the past 2.5 Myr. Nature 365, 829–832.
Guyodo, Y., Valet, J.-P., 1996. Relative variations in geomagnetic intensity from sedimentary records: the past 200,000 years. Earth Planet Sci. Lett. 143, 23–36.
Guyodo, Y., Valet, J.-P., 1999. Global changes in intensity of the earth's magnetic field during the pass 800 kyr. Nature 399, 249–252.
Hamilton, W., 1979. Tectonics of the Indonesian region. U.S. Geol. Surv. Prof. Pap. 1078, 345.
Hatakeyama, T., Kono, M., 2001. Shift of the mean magnetic field values: effect of scatter due to secular variation and errors. Earth Planets Space 53, 31–44.
Hatakeyama, T., Kono, M., 2002. Geomagnetic field model for the last 5 My: time-averaged field and secular variation. Phys. Earth planet. Int. 133, 181–215.
Hinschberger, F., et al., 2001. Magnetic lineation constrains for the back-arc opening of the late Neogene South Banda basin (eastern Indonesia). Tectonophysics 333, 47–59.
Honthaas, C., et al., 1998. A Neogene back-arc origin for the Banda Sea basin: geochemical and geochronological constraints from the Banda Ridges (East Indonesia). Tectonophysics 298, 297–317.
Johnson, C.L., Constable, C.G., 1995. The time-averaged geomagnetic field as recorded by lava flows over the past 5 Myr. Geophys. J. Int. 122, 488–519.
Johnson, C.L., Constable, C.G., 1997. The time-averaged geomagnetic field: global and regional biases for 0–5 Ma. Geophys. J. Int. 131, 643–666.
Johnson, C.L., et al., 2008. Recent investigations of the 0–5 Ma geomagnetic field recorded by lava flows. Geochem. Geophys. Geosyst. 9 (4), doi:10.1029/2007GC001696.
Jolivet, L., Huchon, P., Rangin, C., 1989. Tectonic setting of Western Pacific marginal basins. Tectonophysics 160, 23–47.
Kelly, P., Gubbins, D., 1997. The geomagnetic field over the past 5 millions years. Geophys. J. Int. 128, 315–330.
King, J., Banerjee, S.K., Marvin, J., Ozdemir, O., 1982. A comparison of different magnetic methods for determining the relative grain size of magnetite in nature materials: some results from lake sediments. Earth Planet. Sci. Lett. 59, 404–419.
Kono, M., Tanaka, H., Tsunakawa, H., 2000. Spherical harmonic analysis of paleomagnetic data: the case of linear mapping. J. Geophys. Res. 105, 5817–5833.
Lee, C.S., McCabe, R., 1986. The Banda-Celebes-Sulu basin: a trapped piece of Cretaceous–Eocene Oceanic crust? Nature 322, 51–54.
Lee, T.-Q., 1999. Last 160 ka paleomagnetic directional secular variation record from core MD972151, southwestern South China Sea. TAO 10 (1), 255–264.
McElhinny, M.W., 1973. Paleomagnetism and Plate Tectonics. Cambridge University Press, Cambridge, UK, 358.
McElhinny, M.W., McFadden, P.L., Merrill, R.T., 1996. The time-averaged paleomagnetic field 0–5 Ma. J. Geophys. Res. 101, 25007–25027.
Merrill, R.T., McElhinny, M.W., 1977. Anomalies in the time-averaged paleomagnetic field and their implications for the low mantle. Rev. Geophys. Space Phys. 15, 309–323.
Nishimura, S., Suparka, S., 1990. Tectonics of East Indonesia. Tectonophysics 181, 257–266.
Ryan, W.B.F., 1972. Stratigraphy of late Quaternary sediments in the eastern Mediterrean. In: Stanley, D.J. (Ed.), In the Mediterranean Sea: A Natural Sedimentation Laboratory. Dowden, Hutchinson & Ross, Stroudsburg.
Schneider, D.A., Mello, G.A., 1996. A high-resolution marine sedimentary record of geomagnetic intensity during the Brunhes chron. Earth Planet. Sci. Lett. 144, 297–314.
Tauxe, L., 1993. Sedimentary records of relative paleointensity of the geomagnetic field: theory and practice. Rev. Geophys. 31 (3), 319–354.
Tric, E., et al., 1992. Paleointensity of the geomagnetic field during the last 80,000 years. J. Geophys. Res. 97 (B6), 9337–9351.
Valet, J.-P., Meynadier, L., 1993. Geomagnetic field intensity and reversals during the past four million years. Nature 366, 234–238.
Valet, J.-P., Tauxe, L., Clemens, B.M., 1989. Equatorial and mid-latitude records of the last geomagnetic reversal from the Atlantic Ocean. Earth Planet. Sci. Lett. 94, 371–384.
Wessel, P., Smith, W.H.F., 1998. New improved version of Generic Mapping Tools released. EOS Trans. AGU 79, 579.
Wilson, R.L., 1971. Dipole offset. The time average paleomagnetic field over the past 25 million years. Geophys. J. R. Astr. Soc. 22, 491–504.
Wilson, R.L., McElhinny, M.W., 1974. Investigation of the large scale palaeomagnetic field over the past 25 million years. Eastward shift of the Icelandic spreading ridge. Geophys. J. R. Astr. Soc. 39, 570–586.
Zijderveld, J.D.A., 1967. A.C. Demagnetization of Rocks. Elsevier, New York, pp. 256–286.